

Role of defects in transport through a quantum dot single electron transistor

K. P. Singh,^{a)} Subhalakshmi Lamba, and S. K. Joshi^{b)}
National Physical Laboratory, Dr. K. S. Krishnan Marg, New Delhi 110012, India

Sushil Lamba
Recruitment and Assessment Centre, Lucknow Road, Delhi 110054, India

(Received 7 June 2005; accepted 17 April 2006; published online 26 June 2006)

The effect of a single dotlike defect on the transport through a quantum dot single electron transistor weakly coupled to external leads is studied. It is found that the conductance profile is changed significantly by the quantum mechanical tunneling between the dot and the defect and the interactions between them, both of which are dependent on the distance between the dot and the defect, as also by the morphology of the defect. In particular, we find that even a very small strength of interdot interaction has a major influence on the transport and must be taken into account in device fabrication. © 2006 American Institute of Physics. [DOI: 10.1063/1.2205349]

Semiconductor quantum dots with their discrete energy levels continue to be a subject of intensive research mainly because of their potential for wide-ranging technological application. As it is possible to tune the number of electrons on a dot by varying its electrochemical potential, the dot can be used as a single electron turnstile and an electron pump.^{1,2} Single electron tunneling transistors fabricated from quantum dots, where one can monitor and manipulate the motion of individual electrons, can function as extremely sensitive electrometers.^{3,4} In recent times one has also seen a spurt in investigations of coupled quantum dot systems, with individual dots coupled by both the quantum mechanical tunneling as well as by the interdot Coulomb interactions.⁵ A system of two to three coupled dots with tunable interdot coupling can be used to generate tunable qubit circuits. It is possible to create a two level system from a coupled double dot containing a single electron.⁶ Controlling the electron spin in individual and coupled quantum dots could thus lead to technology for quantum information processing.⁷⁻⁹ Recent theoretical investigations in the parallel coupled two path double quantum dot systems also suggest that forms of correlated behavior can be observed in these systems which are driven by a competition between the Kondo coupling to the leads and the interdot coupling.^{10,11}

A common feature of quantum dot devices is the extreme sensitivity of the device to the surrounding electrostatic environment. The transport through a single dot device can be significantly changed by the presence of a defect in the proximity of the active device as a result of tunneling between the defect and the active device and the interactions between them. Such defects could arise naturally in the process of fabrication of the device or could be introduced deliberately in order to control the properties of the device. Recent studies of the charge transport through a single elec-

tron transistor (SET) with a single fabricated dot, in fact, shows the signature of double dotlike charging behavior¹² indicating the presence of another dot in its vicinity.

In this context we study analytically the effect of a dotlike defect present near a quantum dot single electron transistor which consists of a semiconductor quantum dot weakly coupled to the the source and drain leads and to the gate electrode. The single electron charging properties of such coupled dot systems in a parallel configuration have been experimentally reported by different groups.^{13,14} For the analysis presented here we describe the system using an extended Anderson Hamiltonian and the conductance is calculated using the nonequilibrium Green's function technique. The analysis is valid for temperatures higher than the Kondo temperatures for these systems.¹⁵

Our model system consists of a quantum dot attached to ideal leads, hitherto referred to as dot 1, which represents the SET. A second dot at a distance \mathbf{r} from this dot represents the defect in the system and is referred to as dot 2. A schematic diagram of this model system is shown in the inset of Fig. 1. This double quantum dot system can be described by an (extended) Anderson Hamiltonian as follows:^{16,17}

$$\begin{aligned}
 H = & \sum_{i\sigma} \epsilon_{i\alpha} c_{i\alpha\sigma}^\dagger c_{i\alpha\sigma} + \sum_{\alpha\beta\sigma} \sum_{i \neq j} t_{ij}^{\alpha\beta} c_{i\alpha\sigma}^\dagger c_{j\beta\sigma} \\
 & + \frac{1}{2} \sum_{\alpha\beta} \sum_{\sigma\sigma'} \sum_{ij} U_{ij}^{\alpha\beta} n_{i\alpha\sigma} n_{j\beta\sigma'} + \sum_{k\sigma} \epsilon_k^s s_{k\sigma}^\dagger s_{k\sigma} \\
 & + \sum_{k\sigma} \epsilon_k^d d_{k\sigma}^\dagger d_{k\sigma} + \sum_{k\alpha\sigma} (V_k^s s_{k\sigma}^\dagger c_{1\alpha\sigma} + \text{H.c.}) \\
 & + \sum_{k\alpha\sigma} (V_k^d d_{k\sigma}^\dagger c_{1\alpha\sigma} + \text{H.c.}). \tag{1}
 \end{aligned}$$

The first term of the Hamiltonian represents the energy of an electron in the α th level of the i th dot, with ($i=1,2$) and $c_{i\alpha\sigma}^\dagger$ is the creation operator for an electron with spin σ in the same dot. The second term represents the tunneling between the dots and the third term represents the Coulomb interaction between the electrons (both onsite and interdot) in the

^{a)}Also at Department of Physics, Jamia Millia Islamia, New Delhi 110025, India and on leave from the Directorate of Maize Research, Pusa Campus, New Delhi 110012 India.

^{b)}Electronic mail: skjoshi@mail.nplindia.ernet.in

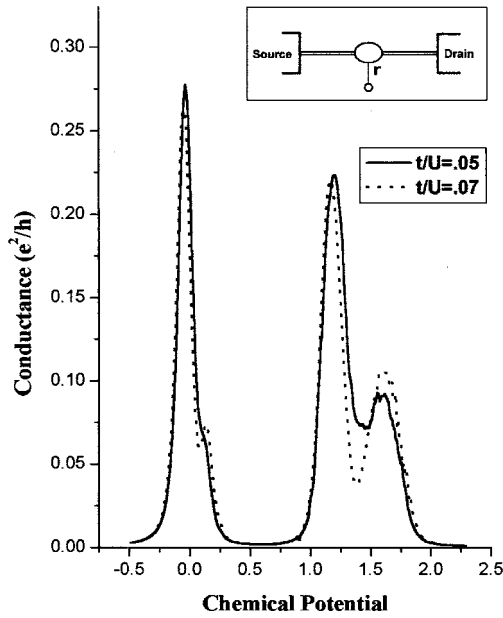


FIG. 1. Variation of conductance with the chemical potential for two different values of the tunneling coefficient and a fixed value of the interdot interaction $g/U=0.08$. The inset shows a schematic diagram of the model system which consists of a quantum dot attached to ideal leads representing the SET and a second (defect) dot at a distance r from this dot.

dots. The next two terms are the energies of the electrons in the leads, where $s_{k\sigma}^\dagger$ and $d_{k\sigma}^\dagger$ are the creation operators for the source and drain, respectively. The last four terms denote coupling terms of dot 1 to the source and drain.

The system conductance is calculated by using Meir's extension¹⁷ of the Landauer formula for interacting systems,

$$G = \frac{e^2}{h} \sum_{\sigma} \int_{-\infty}^{\infty} d\epsilon f_{FD}'(\epsilon) \frac{2\Gamma^{s\sigma}(\epsilon)\Gamma^{d\sigma}(\epsilon)}{\Gamma^{s\sigma}(\epsilon) + \Gamma^{d\sigma}(\epsilon)} \text{Im}[G_{1\sigma}(\epsilon)], \quad (2)$$

where the elastic couplings of the dot 1 to the leads, $\Gamma^{s\sigma}(\epsilon)$ and $\Gamma^{d\sigma}(\epsilon)$, are defined as

$$\Gamma^{s(d)\sigma}(\epsilon) = 2\pi \sum_k |V_{k\sigma}^{s(d)}|^2 \delta(\epsilon - \epsilon_{k\sigma}^{s(d)}), \quad (3)$$

and $G_{1\sigma}(\epsilon)$ is the Fourier transform of the following retarded Green's function pertaining to dot 1,

$$G_{1\sigma}(t) = -i\Theta(t) \langle \{c_{1\sigma}(t), c_{1\sigma}^\dagger(0)\} \rangle = \langle c_{1\sigma}; c_{1\sigma}(0) \rangle. \quad (4)$$

The subscript α on the operators has been dropped by assuming that the dots are small enough so that each dot has just one relevant energy level which is denoted by ϵ_1 for dot 1 and ϵ_2 for dot 2. The onsite Coulomb interaction on both dots $U_{ij}=U_1$ for $i=j=1$, U_2 for $i=j=2$, and the interdot Coulomb interaction $U_{ij}=g$ for $i \neq j$. The tunneling matrix element $t_{ij}=t$. Green's functions for the problem were evaluated by using Keldysh's nonequilibrium Green's function formalism. Green's function is differentiated with time, which leads to higher order Green's functions. At some stage Green's functions must be approximated in order to close the equations. In our calculations all Green's functions containing up to four operators are retained as they are whereas the higher order terms are approximated by the Hartree-Fock approximation. These approximations are valid at temperatures

which are higher than the Kondo temperatures for these systems. In addition to $G_{1\sigma}(t)$, Green's function for the second dot $G_{2\sigma}(t)$ is defined in the same way, and also evaluated by the same approach. This scheme of truncation leads to eight equations for $G_{1\sigma}(t)$. The seven other Green's functions which appear in this scheme are

$$\begin{aligned} G_{3\sigma}(t) &= \langle c_{2\sigma}; c_{1\sigma}^\dagger \rangle, & G_{4\sigma}(t) &= \langle n_{1\bar{\sigma}} c_{1\sigma}; c_{1\sigma}^\dagger \rangle, \\ G_{5,1\sigma}(t) &= \langle n_{2\sigma} c_{1\sigma}; c_{1\sigma}^\dagger \rangle, \\ G_{5,2\sigma}(t) &= \langle n_{2\bar{\sigma}} c_{1\sigma}; c_{1\sigma}^\dagger \rangle, & G_{7\sigma}(t) &= \langle n_{2\bar{\sigma}} c_{2\sigma}; c_{1\sigma}^\dagger \rangle, \\ G_{9,1\sigma}(t) &= \langle n_{1\sigma} c_{2\sigma}; c_{1\sigma}^\dagger \rangle, \\ \text{and } G_{9,2\sigma}(t) &= \langle n_{1\bar{\sigma}} c_{2\sigma}; c_{1\sigma}^\dagger \rangle. \end{aligned}$$

The equations for Green's functions are as follows:

$$\begin{aligned} (\omega - \epsilon_1 - X - Y)G_{1\sigma}(\epsilon) &= 1 + tG_{3\sigma}(\epsilon) + U_1G_{4\sigma}(\epsilon) + g[G_{5,1\sigma}(\epsilon) + G_{5,2\sigma}(\epsilon)], \quad (5) \end{aligned}$$

$$\begin{aligned} (\omega - \epsilon_2)G_{3\sigma}(\epsilon) &= tG_{1\sigma}(\epsilon) + U_2G_{7\sigma}(\epsilon) + g[G_{9,1\sigma}(\epsilon) + G_{9,2\sigma}(\epsilon)], \quad (6) \end{aligned}$$

$$\begin{aligned} [\omega - \epsilon_1 - U_1 - g(\langle n_{2\bar{\sigma}} \rangle + \langle n_{2\sigma} \rangle) - X - Y]G_{4\sigma}(\epsilon) &= \langle n_{1\bar{\sigma}} \rangle + tG_{9,2\sigma}(\epsilon) + g\langle n_{1\bar{\sigma}} \rangle [G_{5,1\sigma}(\epsilon) + G_{5,2\sigma}(\epsilon)], \quad (7) \end{aligned}$$

$$\begin{aligned} [\omega - \epsilon_1 - g(1 + \langle n_{2\bar{\sigma}} \rangle) - X - Y - U_1\langle n_{1\bar{\sigma}} \rangle]G_{5,1\sigma}(\epsilon) &= \langle n_{2\sigma} \rangle + tG_{9,1\sigma}(\epsilon) + \langle n_{2\sigma} \rangle [U_1G_{4\sigma}(\epsilon) + gG_{5,2\sigma}(\epsilon)], \quad (8) \end{aligned}$$

$$\begin{aligned} [\omega - \epsilon_1 - g(1 + \langle n_{2\sigma} \rangle) - X - Y - U_1\langle n_{1\bar{\sigma}} \rangle]G_{5,2\sigma}(\epsilon) &= \langle n_{2\bar{\sigma}} \rangle + tG_{7\sigma}(\epsilon) + \langle n_{2\bar{\sigma}} \rangle [U_1G_{4\sigma}(\epsilon) + gG_{5,1\sigma}(\epsilon)], \quad (9) \end{aligned}$$

$$\begin{aligned} [\omega - \epsilon_2 - U_2 - g(\langle n_{1\bar{\sigma}} \rangle + \langle n_{1\sigma} \rangle)]G_{7\sigma}(\epsilon) &= tG_{5,2\sigma}(\epsilon) + g\langle n_{2\bar{\sigma}} \rangle [G_{9,1\sigma}(\epsilon) + G_{9,2\sigma}(\epsilon)], \quad (10) \end{aligned}$$

$$\begin{aligned} [\omega - \epsilon_2 - g(1 + \langle n_{1\bar{\sigma}} \rangle) - U_2\langle n_{2\bar{\sigma}} \rangle]G_{9,1\sigma}(\epsilon) &= tG_{5,1\sigma}(\epsilon) + \langle n_{1\sigma} \rangle [U_2G_{7\sigma}(\epsilon) + gG_{9,2\sigma}(\epsilon)], \quad (11) \end{aligned}$$

$$\begin{aligned} [\omega - \epsilon_2 - g(1 + \langle n_{1\sigma} \rangle) - U_2\langle n_{2\bar{\sigma}} \rangle]G_{9,2\sigma}(\epsilon) &= tG_{4\sigma}(\epsilon) + \langle n_{1\bar{\sigma}} \rangle [U_2G_{7\sigma}(\epsilon) + gG_{9,1\sigma}(\epsilon)], \quad (12) \end{aligned}$$

where $X = \sum_k |V_k^s|^2 / (\epsilon - \epsilon_k^s)$ and $Y = \sum_p |V_p^d|^2 / (\epsilon - \epsilon_p^d)$. Another eight equations result for $G_{2\sigma}(\epsilon)$. The equations for $G_{1\sigma}(\epsilon)$ and $G_{2\sigma}(\epsilon)$ are solved self-consistently as a function of the chemical potential μ along with the following equations for the average occupation numbers:

$$\langle n_{i\sigma} \rangle = \frac{1}{\pi} \int d\epsilon f_{FD}(\epsilon) \{-\text{Im}[G_{i\sigma}(\epsilon)]\}, \quad i = 1, 2. \quad (13)$$

The conductance as a function of the chemical potential is then calculated from Eq. (2). The implicit equations are solved numerically. We study the conductance for different parameters of the system, which are the difference between

the energy levels on the two dots, the tunneling matrix, the interdot interaction, and the temperature.

The calculations for the conductance are carried out for the paramagnetic case. Hence $\langle n_{i\sigma} \rangle = \langle n_{i\bar{\sigma}} \rangle$ and $G_{i\sigma} = G_{i\bar{\sigma}}$ for both dots. The remaining parameters for the calculation are chosen by keeping in mind the systems which have been studied in experiments. All energies in the calculation are scaled to the onsite charging energy for dot 1, $U_1 = U$.

The conductance of a single quantum dot weakly coupled to ideal leads was studied by Meir *et al.*¹⁷ In our scheme of calculation, in the absence of tunneling and interdot interactions, the results of Ref. 17 are reproduced. If ϵ represents the bare energy level on the dot, then two peaks are seen in the variation of the conductance with chemical potential, which are at ϵ and $\epsilon + U$. The presence of a second dot in the vicinity of this dot modifies this picture considerably. When electrons are able to tunnel coherently between the two dots the eigenstates of the dots which were hitherto localized within the dot get delocalized, extending over the entire double dot system. In a simplified picture, with no interactions between the dots and taking into account only one occupied level in each dot, the system can be treated as a quantum mechanical two level system and it is then possible to calculate exactly the eigenenergies of this system. In this case the energy level of the single dot is now split by the tunneling between the dots into two closely spaced levels. The splitting energy is proportional to the tunneling energy and the difference between the bare energies of the two dots.⁵ Thus it is expected that the single peaks observed at ϵ and $\epsilon + U$ for an ideal SET comprising of a single quantum dot will split into two peaks each for the SET+defect dot system. The position and heights of the peaks are further modified by the interdot Coulomb interaction. Here we report separately and in detail the effects of the variation of the tunneling coefficient, interactions, and the energy level tuning between the dots in the presence of Coulomb interactions on the conductance of the system.

We first study the effect of the change in the interdot tunneling parameter on the conductance with varying chemical potential. The energy levels on the two dots are $\epsilon_1/U = 0$ and $\epsilon_2/U = 0.1$, respectively, $U_2/U = 1$ and $\Gamma^s/U = \Gamma^d/U = 0.025$. Since dot 2 is the defect, it is necessary to ensure that the tunneling matrix element t is much smaller than $V^{s(d)}$, the coupling between the dot and the leads. However, a perceptible change in the conductance behavior of the SET due to the presence of the defect will be observed only when t is larger than the temperature of operation. Otherwise the temperature induced smearing of the conductance peak will mask the effect of the defect. In our studies the temperature is kept fixed at $k_B T/U = 0.03$. It is the smallest parameter in the system and $k_B T < t \ll V^{s(d)} \ll U$. In Fig. 1 we plot the variation of the conductance with the chemical potential for two different values of the interdot tunneling coefficient $t/U = 0.05$ and $t/U = 0.07$, with the interaction strength being kept fixed at $g/U = 0.08$. The single dot peaks at ϵ_1/U and $(\epsilon_1 + U)/U$ are split into two peaks each (the splitting being proportional to the tunneling coefficient), which are now separated by $(U + \Delta)/U$, where Δ is the renormalization of the onsite Coulomb repulsion by the interdot interaction. The

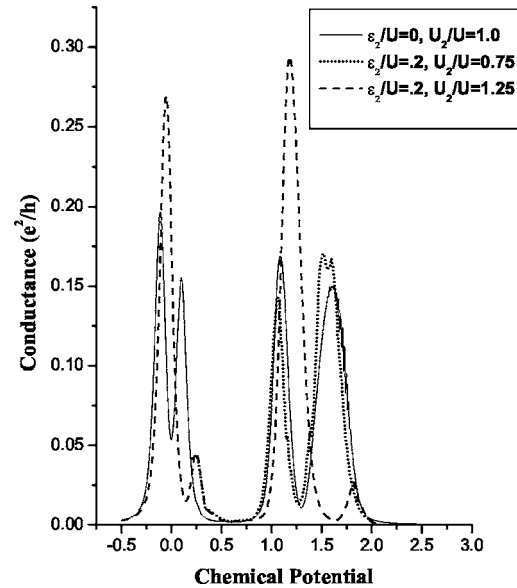


FIG. 2. Variation of conductance with the chemical potential for a perfectly tuned double dot system and for a detuned system for two different values of U_2/U .

peak separation between the first and second peaks, where the interaction effects are not important, is decided entirely by the energy level difference $\epsilon_1 - \epsilon_2$ and the tunneling coefficient t , and tallies with the results for a two level system, which predicts a peak separation $\sim \sqrt{(\epsilon_1 - \epsilon_2)^2 + (2t)^2}$.⁵ The peak separation between the third and fourth peaks is larger than this, which is an effect of interdot interactions. The second and fourth peaks are suppressed compared to the first and third, but the height of these peaks is found to increase as the tunneling strength is increased. The second and fourth peaks indicate the noise that would be recorded in the SET due to the presence of the defect dot.

Tunneling between the dots is enhanced by the increase of the overlap between the wave functions corresponding to the levels ϵ_1 and ϵ_2 which can then be controlled by the distance between the dots. If the distance between the dot and the defect is reduced the noise recorded in the conductance of the SET will increase further, an effect which must either be eliminated or utilized to tailor-make a specific device.

Another parameter that may be expected to influence the transport through the SET is the tuning between the energy levels and the charging energies of the two coupled dots, which would be decided by the morphology of the defect. It is expected that the tuning of the energy levels should lead to the enhanced tunneling of electrons between the two dots. In order to elucidate this point, in Fig. 2 we plot the variation of the conductance with the chemical potential for three different sets of values for ϵ_2/U and U_2/U for a fixed value of $\epsilon_1/U = 0$, $t/U = 0.1$, $g/U = 0.08$, and $k_B T/U = 0.03$. For $\epsilon_2/U = 0$ and $U_2/U = 1$, the two dots are identical and we can see that the heights of the first and second peaks are almost identical, as also of the third and fourth peaks. This is in contrast to the case where the two dots are detuned where the second and fourth peaks are much smaller than the first and third peaks, respectively (Fig. 1). To note the effect of U_2 we have

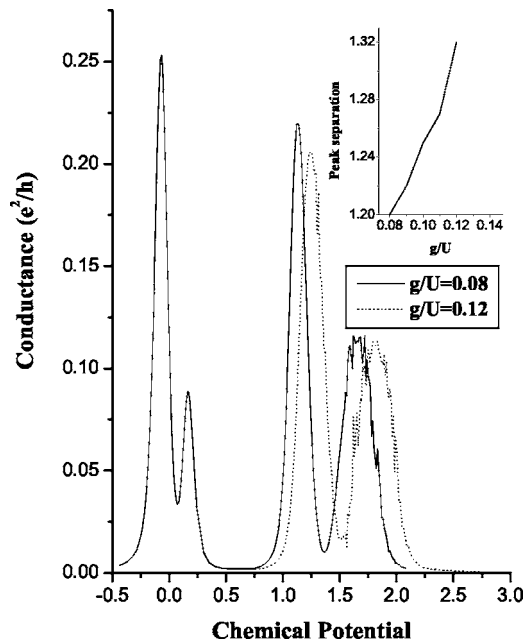


FIG. 3. Variation of conductance with the chemical potential for two different interaction strengths and a fixed value of the tunneling coefficient. The inset shows the variations of the separation between the first and third peaks as a function of interaction strength.

also plotted the conductance for $\epsilon_2/U=0.2$ and $U_2 \neq U$, which is the more likely situation. For $U_2/U=1.25$, the fourth peak is not only at a larger value of the chemical potential but also reduces in weight compared to the third peak. For $U_2/U=0.75$, the defect dot becomes prominent because of its lower charging energy compared to the main dot and the fourth peak actually gains in height compared to the third. Thus it is expected that along with the proximity to the dot, the shape and structure of the defect dot (which in turn controls the energy level spectra and the charging energy, i.e., ϵ_2 and U_2) will also influence the transport through the SET.

In the next figure we study the effects of interdot interactions on the transport through the dots. The energy levels are $\epsilon_1/U=0$ and $\epsilon_2/U=0.1$, respectively, $U_2/U=1$ and $\Gamma^s/U=\Gamma^d/U=0.025$, the temperature $k_B T/U=0.03$ and the tunneling parameter is fixed at $t/U=0.1$. It is seen that, as expected, the first and second peaks are not affected by the change in the interaction strength (Fig. 3). However, there is a significant change in both the position and the width of the third and fourth peaks. With increasing interactions, the third and fourth peaks are shifted to higher chemical potentials due to the renormalization of the onsite Coulomb interaction by the addition of electrons. Both peaks show a broadening

and a reduction in height which indicate that the filling of the third and fourth electrons in the double dot system is inhibited due to the interdot interactions. In the inset we plot the separation between the first and third peaks as a function of interaction strength, which shows an almost monotonic increase when the interaction strength is increased from 0.08 to 0.12. Thus even an interaction strength of the order of $\sim 10\%$ of the onsite Coulomb energy makes a substantial difference in the conductance. Both the tunneling matrix element and the intersite Coulomb interactions can be calculated for a specific device geometry as a function of the intersite separation. This would make it possible to modify the properties of the device by defect engineering.

This study clearly shows how the presence of defects in the vicinity of an active device changes its electrical response. Given that the transport properties of the device are affected not only by the morphology of the neighboring defect but also by the distance between them, which decides the tunneling matrix and the interactions; this study is relevant to understand the limits to the packing density of single electron devices. It is also possible to tailor-make single electron devices with the desired electrical response by incorporating defects of various shapes and sizes.

One of the authors (S.L.) wishes to acknowledge the Council for Scientific and Industrial Research, India, for financial assistance.

- ¹L. P. Kouwenhoven, A. T. Johnson, N. C. Van der Vaart, C. J. P. M. Harmans, and C. T. Foxon, *Phys. Rev. Lett.* **67**, 1626 (1991).
- ²H. Pothier, P. Lafrange, C. Urbina, D. Esteve, and M. H. Devoret, *Europhys. Lett.* **17**, 249 (1992).
- ³L. Zhuang, L. Guo, and S. Y. Chou, *Appl. Phys. Lett.* **72**, 1205 (1998).
- ⁴M. A. H. Khallafalla, Z. A. K. Durrani, and H. Mizuta, *Appl. Phys. Lett.* **85**, 2262 (2004).
- ⁵W. G. van der Wiel, S. De Franceschi, J. M. Elzerman, T. Fujisawa, S. Tarucha, and L. P. Kouwenhoven, *Rev. Mod. Phys.* **75**, 1 (2003).
- ⁶J. R. Petta, A. C. Johnson, C. M. Marcus, M. P. Hanson, and A. C. Gosard, *Phys. Rev. Lett.* **93**, 186802 (2004).
- ⁷D. Loss and D. P. DiVincenzo, *Phys. Rev. A* **57**, 120 (1998).
- ⁸F. Troiani, E. Molinari, and U. Hohenester, *Phys. Rev. Lett.* **90**, 206802 (2003).
- ⁹J. R. Petta *et al.*, *Science* **309**, 2180 (2005).
- ¹⁰R. Aguado and D. C. Langreth, *Phys. Rev. Lett.* **85**, 1946 (2000).
- ¹¹J. C. Chen, A. M. Chang, and M. R. Melloch, *Phys. Rev. Lett.* **92**, 176801 (2004).
- ¹²B. H. Choi, Y. S. Yu, D. H. Kim, S. H. Son, K. H. Cho, S. W. Hwang, D. Ahn, and B. G. Park, *Physica E (Amsterdam)* **13**, 946 (2002).
- ¹³F. Hofmann, T. Heinzel, D. A. Wharam, J. P. Kothaus, G. Bohm, W. Klein, G. Trankle, and G. Weimann, *Phys. Rev. B* **51**, 13872 (1995).
- ¹⁴T. H. Whang and Y. Aoyagi, *Appl. Phys. Lett.* **78**, 634 (2001).
- ¹⁵C. Lacroix, *J. Phys. F: Met. Phys.* **11**, 2389 (1981).
- ¹⁶S. Lamba and S. K. Joshi, *Phys. Rev. B* **62**, 1580 (2000).
- ¹⁷Y. Meir, N. S. Wingreen, and P. A. Lee, *Phys. Rev. Lett.* **66**, 3048 (1991).